Polymer Journal, Vol. 15, No. 10, pp 733—742 (1983)

Packing Disorder in Form II of Poly(vinylidene fluoride): Influence of Elongation and Annealing Temperature

Yasuhiro TAKAHASHI

Department of Macromolecular Science, Osaka University, Toyonaka, Osaka 560, Japan

(Received September 2, 1983)

ABSTRACT: In the crystal structure of poly(vinylidene fluoride) form II, four molecules with different orientation occupy a crystal site with different probabilities. The crystallite of form II gives two kinds of antiphase domain structures, one on the *c*-projection and the other on the *a*-projection. The structural change of form II by elongation and annealing temperature can be explained in terms of the antiphase domain structures and the long- and short-range order parameters. Drawing of the sample produces the domain walls and forms the antiphase domain structure in the crystallite during the recrystallization process. Increasing elongation temperature diminishes the fraction and domain size of the minor component of the antiphase domain structure on the *c*-projection. Annealing below 160°C hardly affects this structure. As the annealing temperature is increased above 166°C, the fraction of the minor component and domain sizes of both minor and major components on the *c*-projection become larger. The disorder on the *a*-projection diminishes with increasing annealing temperature. On the basis of the antiphase domain structure, a mechanism for the change in molecular packing accompanying the transformation from form II to form III is discussed.

KEY WORDS Poly(vinylidene fluoride) / Packing Disorder / Antiphase Domain Structure / Long-Range Order Parameter / Short-Range Order Parameter / Growth Fault / Domain Wall / Superlattice Spot / Inversion Motion / Crystal Phase Transformation / Antipolar-Antiparallel / Polar-Parallel / Form II / Form III / Polar II / Streak II /

A great number of X-ray diffraction studies have been carried out on the disorder in the crystalline region of polymers. Approaches to the disordered structure may be classified into two groups. The first is to determine the so-called statistical structure, in which molecules of different orientation or different chemical structure statistically occupy a crystal site with the same probability. Bunn[1] first proposed the statistical structure for the crystal structure of atactic poly(vinyl alcohol) and Natta *et al.* subsequently found the same type of disorder in many polymers including it-polystyrene,[2] it-polypropylene,[3] it-polybutene-1.[4] The statistical structure can be revealed by crystal structure analysis and represents a long-range order existing in a disordered structure. The second approach is to estimate the paracrystalline disorder proposed and investigated by Hosemann *et al.*[5] This disorder relates the spatial distribution of lattice points to the half-widths of a series of reflections and is described only by the short-range order, *i.e.*, the distribution function of first nearest neighbors.

A third approach to the disorder in polymer crystals is to attempt to describe the short-range order more concretely. In consideration of this, we recently analyzed the X-ray diffuse scattering by poly(vinylidene fluoride),[6-8] and found from the results on streak II and form I that a conformational disorder, a kink band, is contained in the crystalline region. The transformation from form II to form III was attributed to two modes of coorperative motion about the single bonds, *i.e.*, the segmental flip-flop motion and the inversion motion.[9]

Another papers[10,11] on form II poly(vinylidene fluoride) reported the existence of an orientational

packing disorder, in which four molecules with different orientation occupy a crystal site with different probabilities and there exist two kinds of short-range order: antiphase domain structures. From the temperature dependence of the intensity of the superlattice spots of form II, it was found that the reversal of the molecular orientation takes place in the crystalline region at temperatures from 55 to 170°C. This is the temperature range in which molecular motion undergoes an α_c relaxation.[12]

In the present study, the intensities and half-widths of the superlattice spots, which may be related to the long- and short-range order parameters, were measured at various elongation and annealing temperatures to see what structural change occurs in the crystalline region. Furthermore, a mechanism for the change in molecular packing accompanying the phase transformation from form II to form III is proposed.

EXPERIMENTAL

The poly(vinylidene fluoride) sample used for this study was KF-1100 (Kureha Chemical Industry Co., Ltd.). A uniaxially oriented sample of form II was prepared by stretching it at 140, 145, 150, and 155°C in a silicone bath. Annealing was performed for 24 h at intervals of 5°C in the range from 150 to 175°C, after the uniaxially oriented samples prepared by stretching at 150°C were fixed at their ends. The annealed samples were immediately put into petroleum ether. These samples were cut into cubes having the dimensions $0.2 \times 0.2 \times 0.2\,mm^3$ for X-ray measurements.

The X-ray measurements were made using Ni-filtered Cu$K\alpha$ radiation. The intensities and half-widths of the reflections 120 and 130 and the intensity of the reflection 031 were measured using a PSPC (position sensitive proportion counter) system. The profiles of the reflections 120, 130, and 031 for the sample annealed at 170°C are shown in Figure 1.

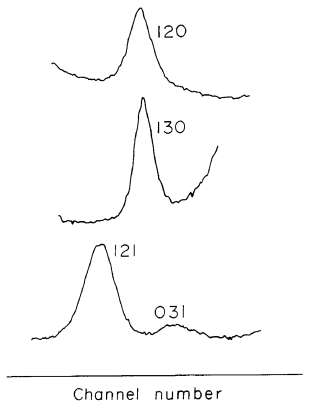

Figure 1. PSPC scans of the reflections 120, 130, and 031 for the sample prepared by annealing at 170°C for 24 h after stretching at 150°C.

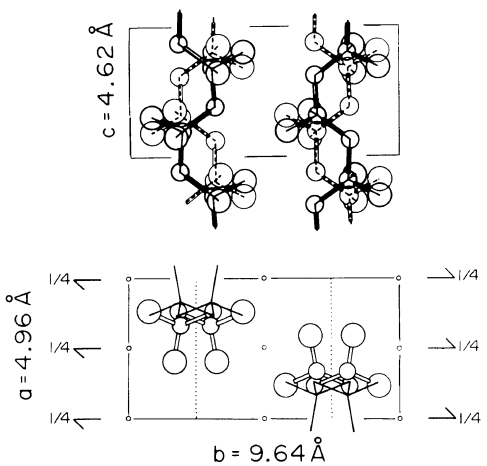

Figure 2. Crystal structure of form II of poly(vinylidene fluoride). Four molecules with different orientation occupy the same crystal site with different probabilities.

RESULTS AND DISCUSSION

Disordered Structure of Form II

In a previous paper,[10] the crystal structure of form II annealed at 175°C for 24 h was analyzed in detail, and it was found that four molecules with different orientations AC, $A\bar{C}$, $\bar{A}C$, and $\bar{A}\bar{C}$ occupy the same crystal site with different probabilities, $w_{AC}=0.54$, $w_{A\bar{C}}=0.29$, $w_{\bar{A}C}=0.10$, and $w_{\bar{A}\bar{C}}=0.07$ (Figure 2). The molecular orientations AC, $A\bar{C}$, $\bar{A}C$, and $\bar{A}\bar{C}$ can be defined by combining the orientations of A and $\bar{A}$ on the c-projection with those of C and $\bar{C}$ on the a-projection. The space group of form II is $P2_1/c$ because of the different probabilities. However, if the four molecules with different orientation have the same probability, the space group should be $Cmcm$.[10] Hence, the hkl reflections with $h+k=2n+1$ correspond to the so-called superlattice spots. On the other hand, from

the half-width relation in the series of reflections $1k0$ and that in the series of reflections $0k1$ we found antiphase domain structures on the c-projection (Figure 4) and for up and down molecules (Figure 5). The two kinds of domains constructing each antiphase domain structure differ in that the origins of the lattices are displaced by $a/2$ and $b/2$. The different orientation probabilities obtained previously for the four molecules by a structure analysis,[10] can be attributed to the difference in the amount of major and minor components of the domains. These antiphase domain structures suggest that the stable local structure of form II is antiparallel and antipolar, which confirms the conclusion reached as early as 1972.[13]

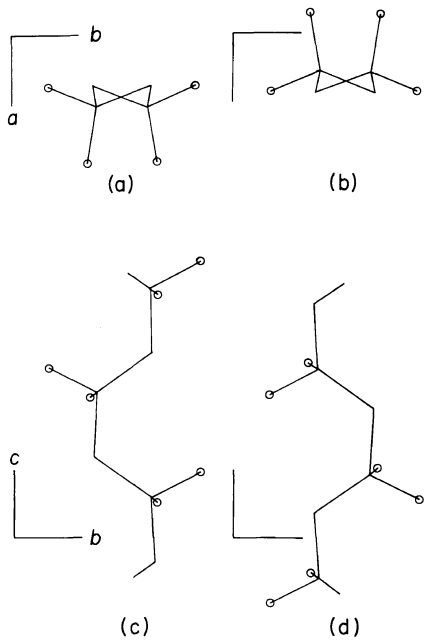

Figure 3. Molecular orientation. (a), (b), (c), and (d) are denoted by the symbols A, $\bar{A}$, C, and $\bar{C}$, respectively. Combinations of the symbols AC, $A\bar{C}$, $\bar{A}C$, and $\overline{AC}$ define molecular orientations.

Diffuse Scattering Intensity Calculation

The diffuse scattering intensity I_2/N in a unit layer structure around the 120 reflection was calculated using the following intensity equation,[11,14]

$$I_2/N = \sum_{\substack{j \\ |\lambda_j|\neq 1}} a_j b_j + \sum_{\substack{j \\ |\lambda_j|\neq 1}} a_j b_j \frac{\lambda_j}{1-\lambda_j} + conj.$$

The *conj.* denotes the complex conjugate of the preceding term. λ_j, a_j, and b_j are defined by,

$$\boldsymbol{Q}_0 = \boldsymbol{O}\boldsymbol{Q}\boldsymbol{O}^{-1}$$

$$\boldsymbol{Q} = \boldsymbol{\Phi}\boldsymbol{P}$$

$$\boldsymbol{Q}_0 = \begin{bmatrix} \lambda_1, & 0, & \cdots, & 0 \\ 0, & \lambda_2, & \cdots, & 0 \\ \cdot & \cdot & & \cdot \\ \cdot & \cdot & & \cdot \\ 0, & 0, & \cdots, & \lambda_n \end{bmatrix}$$

$$\boldsymbol{A} = [a_1, a_2, \cdots, a_n] = \boldsymbol{V}\boldsymbol{F}\boldsymbol{O}^{-1}$$

$$\boldsymbol{B} = [b_1, b_2, \cdots, b_n] = \boldsymbol{V}^*\tilde{\boldsymbol{O}}$$

$$\boldsymbol{V} = [V_1, V_2, \cdots, V_n]$$

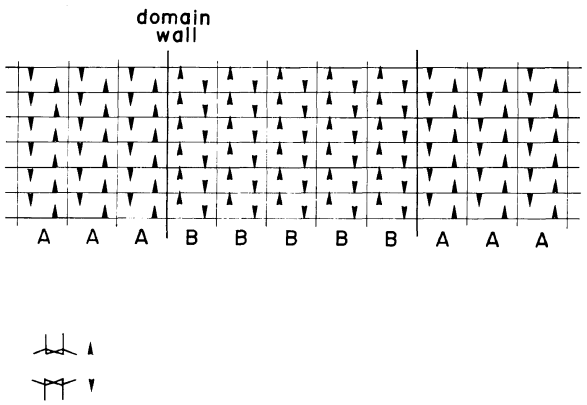

Figure 4. Antiphase domain structure on the c-projection. The origins of two kinds of domains are shifted by $a/2$ and $b/2$ to each other. A and B denote the layer structures used in the diffuse scattering intensity calculation.

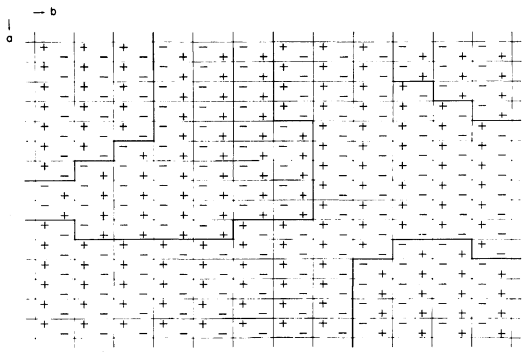

Figure 5. Antiphase domain structure of up and down molecules. The plus and minus denote the up and down molecules, respectively. Bold lines denote domain walls.

$$\boldsymbol{F} = \begin{bmatrix} F_1, & 0, & \cdots, & 0 \\ 0, & F_2, & \cdots, & 0 \\ \cdot & \cdot & & \cdot \\ \cdot & \cdot & & \cdot \\ \cdot & \cdot & & \cdot \\ 0, & 0, & \cdots, & F_n \end{bmatrix}$$

$$\boldsymbol{\Phi} = \begin{bmatrix} e^{-i\phi_1}, & 0, & \cdots, & 0 \\ 0, & e^{-i\phi_2}, & \cdots, & 0 \\ \cdot & \cdot & & \cdot \\ \cdot & \cdot & & \cdot \\ \cdot & \cdot & & \cdot \\ 0, & 0, & \cdots, & e^{-i\phi_n} \end{bmatrix}$$

$$\boldsymbol{P} = \begin{bmatrix} P_{11}, & P_{12}, & \cdots, & P_{1n} \\ P_{21}, & P_{22}, & \cdots, & P_{2n} \\ \cdot & \cdot & & \cdot \\ \cdot & \cdot & & \cdot \\ \cdot & \cdot & & \cdot \\ P_{n1}, & P_{n2}, & \cdots, & P_{nn} \end{bmatrix}$$

where $\boldsymbol{V}^*$ is the complex conjugate of $\boldsymbol{V}$, respectively, $\tilde{\boldsymbol{O}}$ and $\boldsymbol{O}^{-1}$ are the transpose and inverse of $\boldsymbol{O}$, V_j is the layer structure factor of the j-th layer, F_j is the existence probability of the j-th layer, ϕ_j is the phase shift due to the thickness of the layer j, and P_{ij} is the probability of finding the layer j next to the layer i.

The order of the $\boldsymbol{P}$, $\boldsymbol{Q}$, and $\boldsymbol{F}$ matrices is two, since the antiphase domain structure on the c-projection consists of two unit structures A and B. The number of variable parameters can be reduced to two by utilizing the following relations:

$$\sum_j F_j = 1$$

$$\sum_j P_{ij} = 1$$

$$\sum_i F_i P_{ij} = F_j$$

Order Parameters

According to a previous paper,[12] two long-range order parameters S_A and S_C are defined by

$$S_A = 2w_A - 1 \quad (w_A = w_{AC} + w_{A\bar{C}})$$

$$S_C = 2w_C - 1 \quad (w_C = w_{AC} + w_{\bar{A}C})$$

The long-range order parameter is a measure of structural regularity and represents the relative amount of disorder in the structure. Thus, this parameter is unity for a perfectly regular structure and zero for a structure in which the molecules with different orientation have the same existence probability. The parameters S_A and S_C are linearly related to the structure factor ratios $|F_{120}|/|F_{130}|$ and $|F_{031}|/|F_{130}|$, respectively (Figure 6). Here, the structure factor for the reflection 130, F_{130}, was taken as the standard reflection since it is not affected by the orientational disorder.

Another order parameter α, a short-range order parameter, is introduced to describe the regularity of the local structure on the c-projection. This can be related to the parameters used in the diffuse scattering intensity calculation by the following equations:

$$\alpha = 1 - (1 - P_{\mathrm{AA}})/F_{\mathrm{B}} = (P_{\mathrm{AA}} - F_{\mathrm{A}})/F_{\mathrm{B}}$$

$$F_{\mathrm{A}} = w_A$$

$$F_{\mathrm{B}} = 1 - w_A$$

where the subscripts A and B denote the unit structures constructing the antiphase domain structure on the c-projection (Figure 4). The parameter α is zero when $P_{\mathrm{AA}} = F_{\mathrm{A}}$, indicating that no preferable local structure exists. It approaches unity when the structure becomes perfectly regular. This parameter α affects the profile of the superlattice spot on the

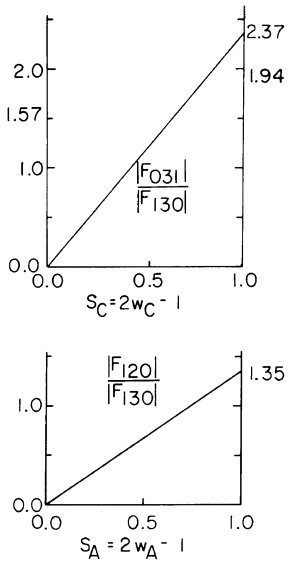

Figure 6. Relationship between the long-range order parameter S_A and the structure factor ratio $|F_{120}|/|F_{130}|$ and that between the long-range order parameter S_C and the structure factor ratio $|F_{031}|/|F_{130}|$.

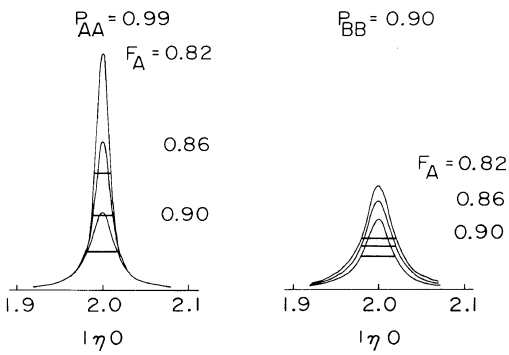

Figure 7. Calculated diffuse scattering intensity profiles around the reflection 120. When $P_{AA}=0.99$, $F_A=0.82$, 0.86, and 0.90 correspond to the short-range order parameter $\alpha=0.944$, 0.929, and 0.900, respectively. When $P_{BB}=0.90$, $F_A=0.82$, 0.86, and 0.90 correspond to the short-range order parameter $\alpha=0.878$, 0.884, 0.889, respectively.

equator, for example, 120. Typical calculated profiles around 120 are shown in Figure 7. In the present study, the difference $\beta_{120}-\beta_{130}$ in half-width between the superlattice spot 120 and the standard reflection 130 was used as a measure of α.

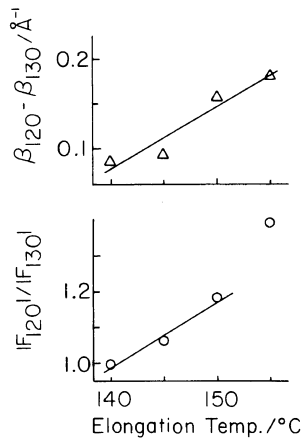

Figure 8. Plots of $|F_{120}|/|F_{130}|$ and $\beta_{120}-\beta_{130}$ against elongation temperature.

Influence of Elongation Temperature

Figure 8 shows that $|F_{120}|/|F_{130}|$ and $\beta_{120}-\beta_{130}$ increase with increasing elongation temperature. Here, the value of $|F_{120}|/|F_{130}|$ at 155°C is less reliable than those at other temperatures because of the lower degree of orientation. The results in Figure 8 indicate that as the temperature is raised, the long-range order parameter S_A increases and the short-range order parameter α decreases. These trends are apparently confusing, showing that the overall structure becomes more regular and the local structure becomes more irregular with increasing elongation temperature. However, a reasonable explanation can be given by considering the antiphase domain structure on the *c*-projection (Figure 4). In Figure 7, the calculated diffuse scattering intensity distribution around 120 is shown for $P_{AA}=0.99$ and $P_{BB}=0.90$. These values of P_{AA} and P_{BB}, which are the probabilities of finding the unit structure A next to A and B next to B, respectively, characterize the relative domain sizes of the major and minor components in the antiphase domain structure. Figure 7 indicates that depending on whether P_{AA} or P_{BB} is constant, the half-width of 120 increases or decreases with increasing F_A or S_A. Figure 8 shows that the long-range order parameter S_A and the half-width increase with increasing elongation temperature. This fact suggests that the fraction and domain size of the minor component become smaller at higher elongation temperature.

Drawing of a bulk polymer induces a series of complex processes, in which recrystallization takes

place after chain unfolding during the transformation from the lamellar or spherulitic crystal to the fibrillar crystal.[15] The growth direction and plane of the fibrillar crystals may be the *b*-axis and (100) plane, respectively, judging from the growth direction and plane of the single crystals[16,17] and spherulites.[18] Therefore, the domain wall may be introduced in the crystallites as a result of dislocation or a growth fault during recrystallization (Figure 9). Furthermore, the fact that the relative amounts of the major and minor components are not equal suggests that a long-range order force plays an important role in the recrystallization process. This force diminishes the domain size of the minor component with increasing elongation temperature. In Figure 10, $|F_{031}|/|F_{130}|$ is plotted against elongation temperature. $|F_{031}|/|F_{130}|$ in-

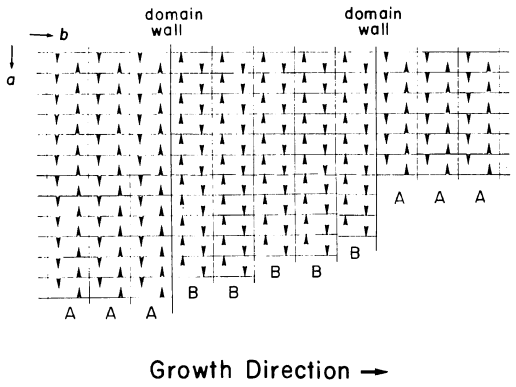

Figure 9. A schematic representation for the recrystallization process during the transformation of the lamellar or spherulitic crystal to the fibrillar crystal. Domain walls are introduced as growth faults.

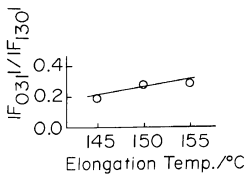

Figure 10. Plots of $|F_{031}|/|F_{130}|$ against elongation temperature.

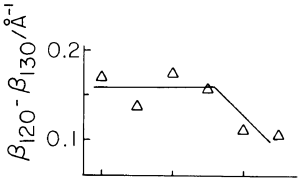

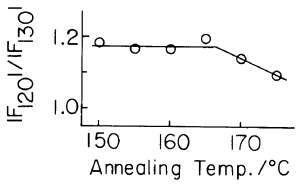

Figure 12. Plots of $|F_{120}|/|F_{130}|$ and $\beta_{120}-\beta_{130}$ against annealing temperature.

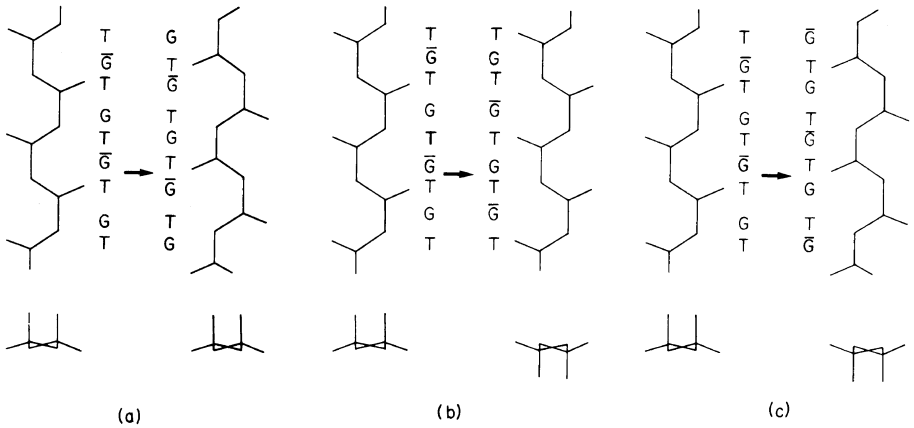

Figure 11. Change in molecular orientation induced by conformational changes about the single bonds. (a), the reversal of the molecule, resulting in α_c relaxation;[12,21] (b), proposed by Lovinger as the mechanism for the transformation from form II to polar II;[22] (c), the inversion essentially the same as in the transformation from form II to form III.[9]

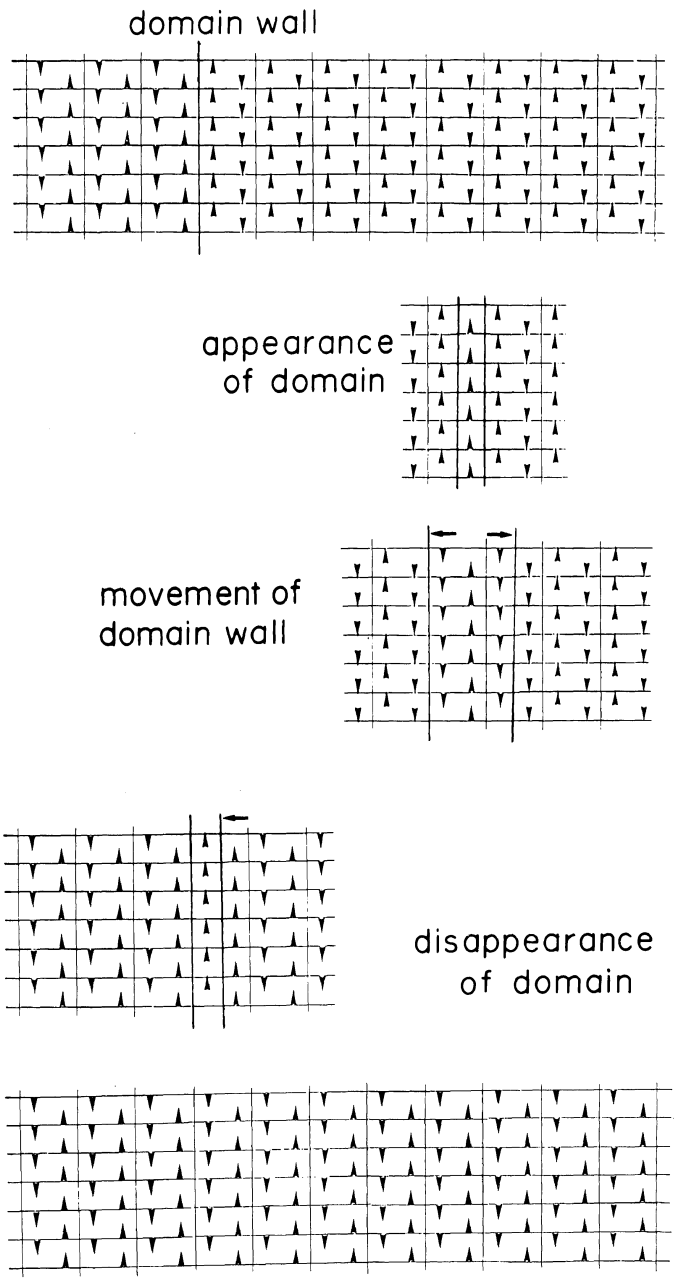

Figure 13. A schematic representation for the appearance, growth, and disappearance of a domain in the antiphase domain structure on the *c*-projection.

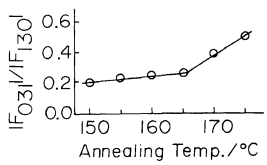

Figure 14. Plots of $|F_{031}|/|F_{130}|$ against annealing temperature.

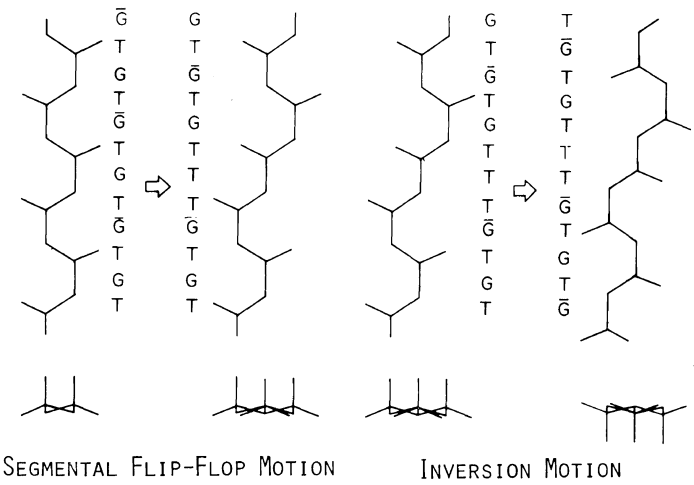

Figure 15. Two modes of molecular motion associated with the crystal phase transformation from form II to form III.

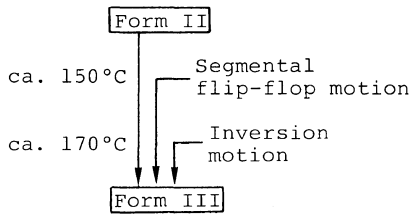

Figure 16. The mechanism for the phase transformation from form II to form III.

creases slightly with increasing elongation temperature, but this should not be taken seriously, if we consider the accuracy of the intensity measurement and the fact that the elongation temperature was in the region where the reversal of the molecular orientation (Figure 11(a)) has been observed.[11]

Influence of Annealing Temperature

Plots of $|F_{120}|/|F_{130}|$ and $\beta_{120}-\beta_{130}$ against annealing temperature are shown in Figure 12. Here, it should be noted that half-widths cannot be measured as accurately as intensities. It can be seen that no change in $|F_{120}|/|F_{130}|$ and $\beta_{120}-\beta_{130}$ occurs below 166°C, but above 166°C, these quantities decrease with increasing annealing temperature. In contrast to the effect of elongation temperature, this behavior indicates that when annealed above 166°C, the structure becomes more regular locally and more irregular as a whole. In other words, the domain sizes of both major and minor components and the fraction of the minor component increase with increasing annealing temperature. Rearrangement of the antiphase domain structure should occur with increasing annealing temperature, since the domain sizes of the major and minor components then increase simultaneously. The movement of the domain wall seems to play an important role in this domain rearrangement. In Figure 13, a model for the appearance, growth, and disappearance of the domain caused by the movement of the domain wall is schematically shown for the antiphase domain structure on the *c*-projection. When the molecules aligned along the *a*-axis change their orientation, a new domain is created. The domain wall moves as a result of the inversion of the molecules aligned along the domain wall. This causes the domain to grow. Finally, the two domain walls coalesce and the domain disappears.

In Figure 14, $|F_{031}|/|F_{130}|$ is plotted against the annealing temperature. The slope is very small below 166°C and becomes steep above 166°C. From the accuracy of the intensity measurement, the slope below 166°C should not be considered significant. Above 166°C, the long-range order parameter S_C increases with increasing annealing temperature, and the structure becomes more regular with respect to the arrangement of up and down molecules. The temperature 166°C agrees with the temperature at which both $|F_{120}|/|F_{130}|$ and $\beta_{120}-\beta_{130}$ begin to decrease. This agreement suggests that the long-range order parameter S_A and short-range order

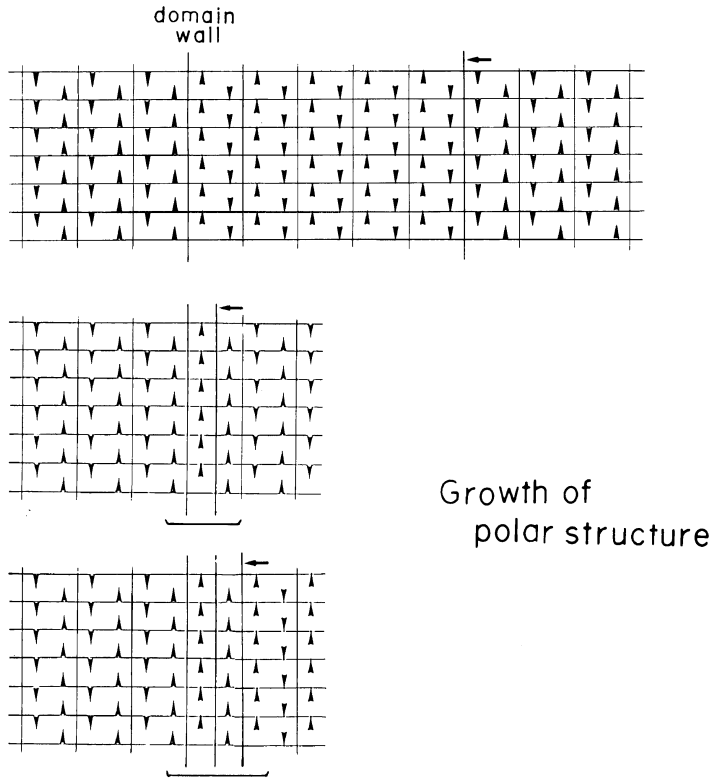

Figure 17. A schematic representation of the mechanism for the change in molecular packing accompanying the transformation from form II to form III.

parameter α are closely related to the long-range order parameter S_C. In other words, the inversion of the molecules (Figure 11(c)), by which the change in molecular orientation from A to $\bar{A}$ occurs simultaneously with that from C to $\bar{C}$ (Figure 3), is induced by heat-treatment. This process should be caused by conformational changes about the single bonds, T to G, T to $\bar{G}$, G to T, and $\bar{G}$ to T. Defect regions may play a role in these changes as in the reverse motion proposed by Miyamoto et al.[21] for the α_c relaxation. The temperature 166°C is consistent with 170°C at which the inversion begins to occur in the transformation from form II to form III.[9]

A Model for the Change in Molecular Packing Accompanying Transformation from Form II to Form III

The mechanism for the transformation from form II to form III *via* streak II was described in the previous paper.[9] The segmental flip-flop motion (Figure 15) begins at about 150°C. As a result of successive introduction of a TT conformation by this motion, the conformation changes gradually from $(TGT\bar{G})_n$ of form II to $(T_3GT_3\bar{G})_n$ of form III. On the other hand, the inversion motion (Figure 15) begins at about 170°C and the molecular packing changes from antipolar-antiparallel for form II to polar-parallel for form III, as schematically shown in Figure 16. During the transformation from form II to form III, the reflections 120 and 130 are broadened and sharpened, respectively, suggesting that the antiphase domain structure appears on the c-projection during the transformation. The mechanism shown in Figure 17 may also be considered for the change in molecular packing during the transformation. There appears a local polar structure on the domain wall. As the domain walls move and coalesce successively, the polar structure grows. In the case of form II, when the domain walls coalesce, the domain disappears, since the polar structure is

less stable. However, during the transformation, the polar structure grows since it is stable because of the molecular conformation being almost $(T_3GT_3\bar{G})_n$. This mechanism is consistent with the following observations on the transformation in the spherulite. Prest and Luca[19] reported for form II that the transformation proceeded radially from the center to the periphery in a way similar to the normal radial growth of a spherulite. On the other hand, Lovinger[20] found that the transformation started at interspherulitic boundaries between forms II and III and proceeded backward to the nucleus. In each case, the transformation proceeds in the radial direction of the spherulite, *i.e.*, along the *b*-axis, starting at the disordered center or periphery of a spherulite. The above-mentioned mechanism for the transformation from form II to form III may also apply to the transformation from form II to polar II caused by an electric field. In this transformation, the molecular packing also changes from antipolar to polar, and the polar structure is stabilized by the electric field.

Acknowledgement. The author expresses his sincere appreciation to Prof. H. Tadokoro for encouragement throughout the course of this research.

REFERENCES

1. C. W. Bunn, *Nature*, **161**, 929 (1948).
2. G. Natta and P. Corradini, *Makromol. Chem.*, **16**, 77 (1955).
3. G. Natta and P. Corradini, *Nuovo Cimento, Suppl.*, **15**, 40 (1960).
4. G. Natta, P. Corradini, and I. W. Bassi, *Nuovo Cimento, Suppl.*, **15**, 52 (1960).
5. R. Hosemann and S. N. Bagchi, "Direct Analysis of Diffraction Matter," North-Holland, Amsterdam, 1962.
6. Y. Takahashi, M. Kohyama, and H. Tadokoro, *Macromolecules*, **9**, 870 (1976).
7. Y. Takahashi and H. Tadokoro, *Macromolecules*, **13**, 1316 (1980).
8. Y. Takahashi, H. Tadokoro, and A. Odajima, *Macromolecules*, **13**, 1318 (1980).
9. Y. Takahashi, Y. Matsubara, and H. Tadokoro, *Macromolecules*, **15**, 334 (1982).
10. Y. Takahashi, Y. Matsubara, and H. Tadokoro, *Macromolecules*, in press.
11. Y. Takahashi and H. Tadokoro, *Macromolecules*, in press.
12. Y. Takahashi and K. Miyaji, *Macromolecules*, in press.
13. R. Hasegawa, Y. Takahashi, Y. Chatani, and H. Tadokoro, *Polym. J.*, **3**, 600 (1972).
14. J. Kakinoki and Y. Komura, *Acta Crystallogr.*, **19**, 137 (1965).
15. A. Peterlin, *J. Mater. Sci.*, **6**, 490 (1971).
16. K. Okuda, T. Yoshida, M. Sugita, and M. Asahina, *J. Polym. Sci., B*, **5**, 465 (1967).
17. K. Sakaoku and A. Peterlin, *J. Macromol. Sci., Phys.*, **1**, 401 (1967).
18. A. J. Lovinger and T. T. Wang, *Polymer*, **20**, 725 (1979).
19. W. M. Prest, Jr. and D. J. Luca, *J. Appl. Phys.*, **46**, 4136 (1975).
20. A. J. Lovinger, *Polymer*, **21**, 1317 (1980).
21. Y. Miyamoto, H. Miyaji, and K. Asai, *J. Polym. Sci., Polym. Phys. Ed.*, **18**, 597 (1980).
22. A. J. Lovinger, *Macromolecules*, **14**, 225 (1981).